



Scale-Invariant Correlations in Dynamic Bacterial Clusters

Xiao Chen,¹ Xu Dong,¹ Avraham Be'er,² Harry L. Swinney,³ and H. P. Zhang^{1,*}

¹*Department of Physics and Institute of Natural Sciences, Shanghai Jiao Tong University, China*

²*Zuckerberg Institute for Water Research, Ben-Gurion University of the Negev, Israel*

³*Center for Nonlinear Dynamics and Department of Physics, University of Texas at Austin, Austin, Texas 78712, USA*

(Received 7 November 2011; published 5 April 2012)

In *Bacillus subtilis* colonies, motile bacteria move collectively, spontaneously forming dynamic clusters. These bacterial clusters share similarities with other systems exhibiting polarized collective motion, such as bird flocks or fish schools. Here we study experimentally how velocity and orientation fluctuations within clusters are spatially correlated. For a range of cell density and cluster size, the correlation length is shown to be 30% of the spatial size of clusters, and the correlation functions collapse onto a master curve after rescaling the separation with correlation length. Our results demonstrate that correlations of velocity and orientation fluctuations are scale invariant in dynamic bacterial clusters.

DOI: 10.1103/PhysRevLett.108.148101

PACS numbers: 87.18.Gh, 05.40.-a, 47.63.Gd

Collective motion can be found in systems of self-propelled objects ranging from flocking birds [1,2] and fish schools [3] to vibrating granular matter [4–6], and even to the microscopic scales of swarming bacteria [7–10] and molecular motors [11–13]. Despite differences in the length scales and the cognitive abilities of constituent individuals, collective motion in these systems produces similar patterns of extended spatiotemporal coherence, suggesting general principles of collective motion. A fruitful approach to unveil these principles has been to model individuals as interacting self-propelled particles, which align their motions with neighbors [14–18]. If the noise level is low enough, local alignment of individual motions can lead to the emergence of long-range order, analogous to the formation of a ferromagnetic phase from local spin interactions. Similar ideas have also been formulated in continuum theories [19–23], and experiments have verified some of the theoretical predictions, such as giant number fluctuations [4,6,10].

Besides exhibiting self-organized global order, flocks, schools, and swarms are highly responsive to external stimuli [1,2,24]. Cavagana *et al.* [2] analyzed the response of flocks of starlings using the fluctuation-dissipation theorem idea to compute spatial correlation functions for small local fluctuations about the ordered state. They found that the correlation lengths of velocity and speed fluctuations within a flock increase linearly with the spatial size of the flock; i.e., the fluctuations are scale invariant. Similar results have also been obtained for bird flocks from simulations of self-propelled particles [25]. Recently Bialek *et al.* used a maximum entropy model, calibrated by observed local correlations in bird flocks, to reproduce long-range scale-invariant correlations [26]; this led to the hypothesis that bird flocks may be poised at criticality [24].

In this Letter, we examine the existence of scale-invariant correlations [2,25,26] in a bacterial system. Our experiments are carried out in colonies of wild-type

Bacillus subtilis 3610 grown on Luria broth agar substrates. For inoculation, 5 μ L of *B. subtilis* overnight culture (optical density at 650 nm = 1) is placed on the agar. The inoculated gel is stored in an incubator at 30 °C and 90% humidity. After a lag time of 2 h, a colony starts to expand outward isotropically with a speed 1.4 cm/hour [10]. After expanding for 1.5 h, the colony (2.1 cm in radius) is placed under an optical microscope (Olympus IX50 with an LD 60X Phase contrast PH2 objective) for measurements. The imaging window (90 \times 90 μ m²) is positioned initially at the edge of the colony, and its position in the laboratory reference frame is left unchanged throughout the experiments. As the colony expands, the average number of bacteria in the field of view N_{total} increases from 343 to 720 in 35 min, and then saturates [10]. At each density condition, we record a video at 60 frame/s for 100 s, during which the increase in N_{total} is only a few percent (2.5% under the density condition of Fig. 1), and the system is in a quasistationary state, as shown by time series records in the Supplemental Material [27].

A typical image of bacteria [10,28] is shown in Fig. 1(a). The bacteria aggregate in dynamic clusters that continually gain and lose members as they move. We determine the position, orientation, and velocity of more than 95% of the bacteria in each image, and successive images are analyzed to extract quantitative information on the evolution of clusters, which typically contain a hundred bacteria [10]. We define two neighboring bacteria as members of the same cluster if their centers of mass are separated by less than a distance R and if their motion directions differ by less than an angle α . In most of our analyses we use $R = 3.6 \mu$ m and $\alpha = 20^\circ$, but the analysis of correlation functions in the Supplemental Material [27] shows that our results depend only weakly on the particular values of R and α around the chosen values. A dynamic cluster is defined to include all bacteria that are connected to at least

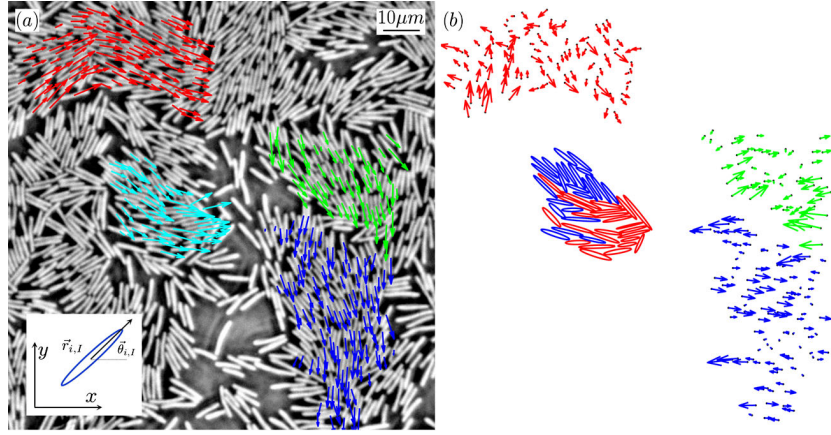


FIG. 1 (color online). (a) Instantaneous velocity vectors of bacteria in four clusters, overlaid on an experimental image where the white rods are individual bacteria; the insert shows schematically the position $\vec{r}_{i,I}$ and orientation, $\tilde{\theta}_{i,I}$ of the i th bacterium in the I th cluster. (b) Fluctuations from the mean motion direction, mean orientation, and mean velocity are shown by arrows for the red, green, and blue clusters. For the cyan cluster in (a), positive and negative speed fluctuations from the mean are shown by red and blue ellipses, respectively. Each cluster has regions of correlated fluctuations with opposite signs (cf. left and right halves of the green cluster). The blue, green, red, and cyan clusters in (a) contain 106, 57, 98, and 48 bacteria, respectively, with corresponding polarizations 0.98, 0.97, 0.91, and 0.94, and cluster sizes 43.2, 33.7, 40.2, and 25.7 μm . The temporally averaged number of bacteria in the imaging window (1000×1000 pixels) is $N_{\text{total}} = 720$. The temporal evolution of these clusters is shown in the Supplemental Material [27].

one other bacterium that satisfies the local distance and motion direction criteria. We use lower-case letters (i or j) to denote bacteria and upper-case letters (I or J) to index clusters. For example, I th cluster contains n_I bacteria, among which the i th ($i \in [1, n_I]$) bacterium is located at $\vec{r}_{i,I}$ and has orientation $\tilde{\theta}_{i,I}$ and velocity $\vec{v}_{i,I}$. The motion of a bacterium is typically in a direction that is close to but not the same as the direction of its body axis. The angle between the body orientation $\tilde{\theta}_{i,I}$ and the velocity direction $\frac{\vec{v}_{i,I}}{|\vec{v}_{i,I}|}$ averaged over all bacteria at all densities, has a mean absolute value of 18 degrees.

We define cluster size as the maximum distance between two bacteria belonging to the same cluster: $L_I = \max\{|\vec{r}_{i,I} - \vec{r}_{j,I}|, i, j \in [1, n_I]\}$ [2]. Cluster size is strongly related to the number of constituent bacteria, as shown in Fig. 2(a), which is obtained in an analysis of more than 10^5 clusters in a field of view with an average of $N_{\text{total}} = 720$ bacteria. We find that the cluster size scales approximately as a power law for $L > 10 \mu\text{m}$, $L = Cn^\varepsilon$; however, variations in the data (as shown by the error bars) lead to a large uncertainty in the power exponent: $\varepsilon = 0.60 \pm 0.13$, meaning that bacterial density within a cluster depends weakly on its size, consistent with results in [10]. Figure 2(b) shows that the number of observed clusters of a given size decreases with cluster size and that the probability of finding large clusters grows markedly with increasing bacterial density. The largest clusters that we observed in significant numbers are about 60 μm in size. In the Supplemental Material [27] we show that the data in Fig. 2(b) can be described by an expression derived from the relation between L and n extracted from Fig. 2(a) and an expression presented in [10] for the probability of

finding a cluster with n bacteria. We note that the increase of typical cluster size shown in Fig. 2(b) may also be explained by a coarsening process as shown in [17].

We determine for each cluster I its mean velocity $\vec{V}_I = \langle \vec{v}_{i,I} \rangle_i$, speed $S_I = \langle |\vec{v}_{i,I}| \rangle_i$, motion direction $\vec{P}_I = \langle \frac{\vec{v}_{i,I}}{|\vec{v}_{i,I}|} \rangle_i$, and orientation $\tilde{\Theta}_I = \langle \tilde{\theta}_{i,I} \rangle_i$, where $\langle \cdot \rangle_i$ denotes an average over all n_I bacteria in the I th cluster. The degree of motion coordination is given by a scalar order parameter, $P_I = |\vec{P}_I|$ [2,16]. If bacteria are perfectly coordinated (all moving in the same direction), $P = 1$, while for random motion, $P = 0$. Our bacterial clusters are highly coordinated in motion: $P = 0.97$ on average, but this collective motion within the clusters does not lead to global order at the colony level, possibly due to hydrodynamic instabilities [19,29,30].

We further compute fluctuations of motion direction, velocity, speed, and orientation: $\vec{d}_{i,I} = \frac{\vec{v}_{i,I}}{|\vec{v}_{i,I}|} - \vec{P}_I$, $\vec{u}_{i,I} = \vec{v}_{i,I} - \vec{V}_I$, $s = s_{i,I} - S_I$, and $\vec{\phi}_{i,I} = \tilde{\theta}_{i,I} - \tilde{\Theta}_I$, respectively. All fluctuations exhibit extended spatial correlations, as shown in Fig. 1(b). To be quantitative, we compute spatial correlations of fluctuations within the I th cluster. For velocity fluctuations, we have

$$C_I^u(r) = \frac{1}{C_0^u} \frac{\sum_{ij} (\vec{u}_{i,I} \cdot \vec{u}_{j,I}) \delta(r - |\vec{r}_{i,I} - \vec{r}_{j,I}|)}{\sum_{ij} \delta(r - |\vec{r}_{i,I} - \vec{r}_{j,I}|)}, \quad (1)$$

where δ is a Dirac function, \sum_{ij} represents the summation over all possible bacterial pairs in the I th cluster and C_0^u is a normalization factor such that $C_I^u(0) = 1$. Our correlation functions are different from those computed in previous

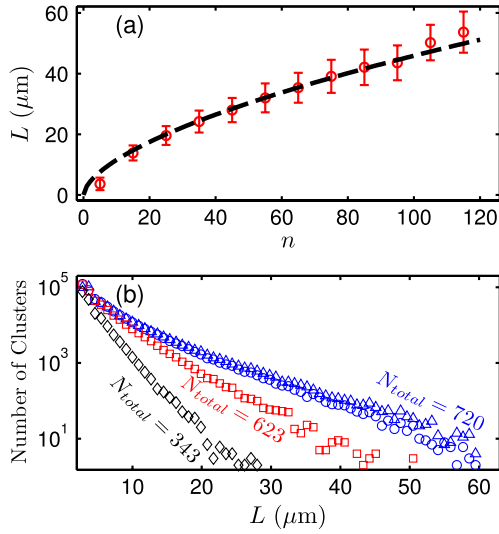


FIG. 2 (color online). (a) Cluster size as a function of the number of bacteria in a cluster. The dashed line is a fit to the data, $L = 2.89n^{0.6}$, where L is averaged in bins of width $\Delta n = 6$ and the error bars represent the standard deviation in each bin. (b) Number of clusters as a function of their size L , for different average numbers of bacteria in a fixed field of view. Neighboring bacteria are identified as belonging to the same cluster if they are closer together than $R = 3.6 \mu\text{m}$ and move in the same direction within $\alpha = 20^\circ$, except for the blue triangles where $R = 4.1 \mu\text{m}$ and $\alpha = 15^\circ$. The results for $N_{\text{total}} = 720$ for two sets of parameters R and α differ only slightly.

studies of bacterial collective motion [7–9]: Eq. (1) averages *within* each cluster, while the correlation functions in [7–9] were averaged *globally* over the whole measurement area. Further, previous work [7–9] used particle image velocimetry to measure velocity fields on fixed grid points instead of tracking individual bacteria. Though the measured velocity fields clearly demonstrated collective motion, the lack of velocity and position information for individual bacteria prevented previous studies from identifying dynamic clusters and from comparing correlation length to cluster size for individual clusters; these are necessary steps to assess the possible existence of scale-invariant correlations. Globally averaged correlation functions of bacterial velocities in a previous study [7] yielded a correlation length ($\sim 15 \mu\text{m}$) and correlation time (~ 0.5 sec) that are similar to our results in [10]. Therefore, the global dynamics of collective motion in these studies share similarities, though differences do exist. For example, the angle between bacterial motion and its body axis in our experiments is smaller than that in [8]. This is possibly related to the fact that bacteria in our experiments swim in a thin film on a no-slip solid substrate, which inhibits advective fluid flow created by neighbors.

To improve statistics, we further average $C_I^u(r)$ over all clusters of size L ,

$$C^u(r; L) = \langle C_I^u(r) \rangle_{L_I=L}. \quad (2)$$

Similarly defined correlation functions of motion direction, speed, and orientation fluctuations are denoted $C^d(r; L)$, $C^s(r; L)$, and $C^\phi(r; L)$, respectively [27]. The four kinds of correlation functions are shown in Fig. 3, where each panel includes results from three cluster sizes and three densities. The correlation functions are not defined for $r < 1 \mu\text{m}$, an excluded-volume region determined by the size of the bacteria. All the correlation functions are positive at short separations and negative at large separations. This is consistent with Fig. 1(b), where there are regions of correlated fluctuations with opposite signs, such as the left and right halves of the cluster at the upper left corner. A good measure of the size of a correlated domain is the value of r where the correlation function passes through zero [2], as shown, for example, by the crosses on the top curve in each panel on the left in Fig. 3; we define the correlation length

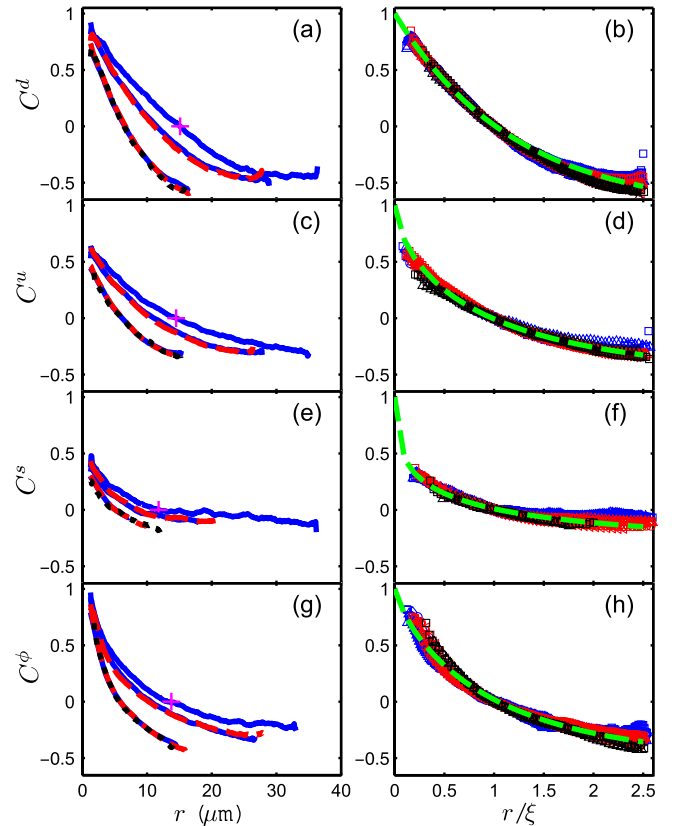


FIG. 3 (color online). Correlation functions of motion direction, (a) and (b); velocity, (c) and (d); speed, (e) and (f); and orientation, (g) and (h). The correlation functions are plotted as a function of r on the left and as a function of r/ξ on the right, where the correlation length ξ was determined from the zero crossings of the left-hand correlation functions, for three cluster sizes ($L = 18.5 \mu\text{m}$, $36.5 \mu\text{m}$, and $54.5 \mu\text{m}$, from left to right in each left-hand panel). The dashed lines in the right-hand plots are stretched-exponential fits, described in the Supplemental Material [27]. The data correspond to bacterial densities $N_{\text{total}} = 343$, 623 , and 720 , and cluster sizes L from $12.5 \mu\text{m}$ to $50.8 \mu\text{m}$.

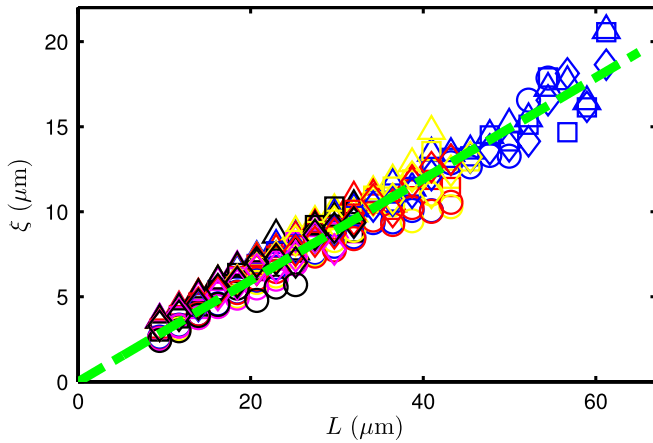


FIG. 4 (color online). Motion direction (ξ^d , Δ), velocity (ξ^u , \square), speed (ξ^s , \circ), and orientation (ξ^ϕ , \diamond) correlation length are plotted as functions of cluster spatial size, L . Results from five densities are shown: $N_{\text{total}} = 343$ (black), $N_{\text{total}} = 480$ (magenta), $N_{\text{total}} = 623$ (red), $N_{\text{total}} = 674$ (yellow) and $N_{\text{total}} = 720$ (blue). All quantities are linearly proportional to L , as demonstrated by green dashed lines: $\xi = 0.3L$. Correlation lengths depend weakly on the parameters (R and α) used to identify clusters as shown in the Supplemental Material [27].

ξ by such zero crossings. The correlation functions on the left of Fig. 3 are plotted on the right as a function of r/ξ . This rescaling leads to a collapse of the correlation functions onto master curves described by stretched exponential fits (cf. Supplemental Material). This indicates that domains of correlated fluctuations in the bacterial clusters have quantitatively similar internal structures. The four different correlation functions all yield correlation lengths that are well represented by $\xi = 0.3L$ (Fig. 4). Thus the correlations in bacterial clusters are long ranged and scale invariant: the range of correlations is not set by any characteristic length scale apart from the size of the cluster. For a wide range in parameters, there is only a weak dependence of ξ on bacterial density and the criteria used to extract clusters, as Fig. 4 and supporting Fig. 4 of the Supplemental Material show.

Long-range scale-invariant correlations have been previously reported in experimental [2], numerical [25], and theoretical [26] studies of bird flocks. In those studies, researchers found that correlation lengths were 35% [2] to 40% [25] of the flock sizes and that correlation functions collapsed after rescaling. Besides being 6 orders of magnitude larger in length scale than bacterial clusters, bird flocks are different in at least three other aspects. First, while interaction between birds depends possibly on topological separation [1,31], bacteria interact through hydrodynamic [30,32–34] and excluded-volume [25,35,36] interactions and through physical intertwining of flagella of neighboring bacteria [9,37,38], which all depend on the metric separation between individuals. Second, interaction between bird flocks are rare because flocks

are usually isolated or well separated, while bacterial clusters often interact with one another, which leads to frequent cluster splitting and merging. Third, birds in flocks move in three dimensions while bacterial motions are confined on a surface. Despite these qualitative differences, long-range scale-invariant correlations are observed in both systems, which suggests that such correlations may be a general feature of systems exhibiting collective motion.

Researchers have hypothesized that systems moving collectively may be poised at a *nonequilibrium critical state* to achieve long-range scale-invariant correlations [2,24]. In a physical system with global order caused by a spontaneously broken symmetry, fluctuations transverse to the order parameter may display scale-invariant correlations, such as Goldstone modes in ferromagnetism; for these soft modes, scale-invariant correlations are a consequence of spontaneous symmetry breaking. However, in models for collective motion [2,24], speed (the analog of modulus of the spins) is regarded as a stiff mode since it does not correspond to any obvious symmetry. The fact that speed also exhibits scale free correlations, thus, is a strong evidence that the system indeed is close to criticality.

Long-range scale-invariant correlations may give some evolutionary advantages [2,24]. With such correlations, a change in the state of an individual influences that of all others in the system; information of an external stimulus, such as a predator or food, can propagate quickly through the whole system and the system can respond coherently to maintain its integrity. From theoretical and modeling perspectives, long-range scale-invariant correlations may serve as a system feature to benchmark existent models and guide future model development [26].

In conclusion, we have identified dynamic clusters based on *local* information of bacterial position and motion direction, and then we investigated spatial correlations of motion direction, velocity, speed, and orientation fluctuations in clusters with sizes ranging from 10 to 60 μm , for mean densities varying by a factor of 2. All fluctuations are found to exhibit long-range correlations, and the ratio of correlation length to cluster size is scale invariant ($\xi/L \approx 0.3$). Correlation functions computed for various conditions collapse onto master curves when separations are rescaled by the corresponding correlation length. Our work together with previous studies on bird flocks suggests that long-range scale-invariant correlations may be a general feature in systems exhibiting collective motion.

We thank David Cai, Xiangjun Xing, and Cheng Tai for useful discussions. We are grateful to D.B. Kearns for providing the bacterial strain and the growth protocol. H.P.Z. acknowledges financial support of the National Natural Science Foundation of China through Grant No. 11104179.

- *To whom correspondence should be addressed: hepeng_zhang@sjtu.edu.cn
- [1] M. Ballerini, N. Calibbibo, R. Candeleir, A. Cavagna, E. Cisbani, I. Giardina, V. Lecomte, A. Orlandi, G. Parisi, A. Procaccini, M. Viale, and V. Zdravkovic, *Proc. Natl. Acad. Sci. U.S.A.* **105**, 1232 (2008).
- [2] A. Cavagna, A. Cimarelli, I. Giardina, G. Parisi, R. Santagati, F. Stefanini, and M. Viale, *Proc. Natl. Acad. Sci. U.S.A.* **107**, 11865 (2010).
- [3] N. C. Makris, P. Ratilal, D. T. Symonds, S. Jagannathan, S. Lee, and R. W. Nero, *Science* **311**, 660 (2006).
- [4] V. Narayan, S. Ramaswamy, and N. Menon, *Science* **317**, 105 (2007).
- [5] A. Kudrolli, G. Lumay, D. Volfson, and L. S. Tsimring, *Phys. Rev. Lett.* **100**, 058001 (2008).
- [6] J. Deseigne, O. Dauchot, and H. Chate, *Phys. Rev. Lett.* **105**, 098001 (2010).
- [7] C. Dombrowski, L. Cisneros, S. Chatkaew, R. E. Goldstein, and J. O. Kessler, *Phys. Rev. Lett.* **93**, 098103 (2004).
- [8] A. Sokolov, I. S. Aranson, J. O. Kessler, and R. E. Goldstein, *Phys. Rev. Lett.* **98**, 158102 (2007).
- [9] H. P. Zhang, A. Be'er, R. S. Smith, E. L. Florin, and H. L. Swinney, *Europhys. Lett.* **87**, 48011 (2009).
- [10] H. P. Zhang, A. Be'er, E. L. Florin, and H. L. Swinney, *Proc. Natl. Acad. Sci. U.S.A.* **107**, 13626 (2010).
- [11] F. J. Nedelec, T. Surrey, A. C. Maggs, and S. Leibler, *Nature (London)* **389**, 305 (1997).
- [12] V. Schaller, C. Weber, C. Semmrich, E. Frey, and A. R. Bausch, *Nature (London)* **467**, 73 (2010).
- [13] X. Q. Shi and Y. Q. Ma, *Proc. Natl. Acad. Sci. U.S.A.* **107**, 11709 (2010).
- [14] C. W. Reynolds, *Comput. Graph.* **21**, 25 (1987).
- [15] I. D. Couzin and J. Krause, *Advances in the Study of Behavior* **32**, 1 (2003).
- [16] T. Vicsek, A. Czirok, E. Benjacob, I. Cohen, and O. Shochet, *Phys. Rev. Lett.* **75**, 1226 (1995).
- [17] H. Chate, F. Ginelli, G. Gregoire, and F. Raynaud, *Phys. Rev. E* **77**, 046113 (2008).
- [18] F. Peruani, T. Klaus, A. Deutsch, and A. Voss-Boehme, *Phys. Rev. Lett.* **106**, 128101 (2011).
- [19] R. A. Simha and S. Ramaswamy, *Phys. Rev. Lett.* **89**, 058101 (2002).
- [20] J. Toner, Y. H. Tu, and S. Ramaswamy, *Ann. Phys. (N.Y.)* **318**, 170 (2005).
- [21] A. W. C. Lau and T. C. Lubensky, *Phys. Rev. E* **80**, 011917 (2009).
- [22] A. Baskaran and M. C. Marchetti, *Proc. Natl. Acad. Sci. U.S.A.* **106**, 15567 (2009).
- [23] S. Ramaswamy, *Annu. Rev. Condens. Matter Phys.* **1**, 323 (2010).
- [24] T. Mora and W. Bialek, *J. Stat. Phys.* **144**, 268 (2011), 10.1007/s10955-011-0229-4.
- [25] C. K. Hemelrijk and H. Hildenbrandt, *PLoS ONE* **6**, e22479 (2011).
- [26] W. Bialek, A. Cavagna, I. Giardina, T. Mora, E. Silvestri, M. Viale, and A. Walczak, *arXiv:1107.0604*.
- [27] See Supplemental Material at <http://link.aps.org/supplemental/10.1103/PhysRevLett.108.148101> for growth protocol, temporal evolutions of clusters, and sensitivity test of parameters used to identify clusters and for more information on the Supplemental Material.
- [28] D. B. Kearns and R. Losick, *Mol. Microbiol.* **49**, 581 (2004).
- [29] H. Chate, F. Ginelli, G. Gregoire, F. Peruani, and F. Raynaud, *Eur. Phys. J. B* **64**, 451 (2008).
- [30] D. Saintillan and M. J. Shelley, *Phys. Rev. Lett.* **99**, 058102 (2007).
- [31] F. Ginelli and H. Chate, *Phys. Rev. Lett.* **105**, 168103 (2010).
- [32] J. P. Hernandez-Ortiz, C. G. Stoltz, and M. D. Graham, *Phys. Rev. Lett.* **95**, 204501 (2005).
- [33] T. Ishikawa and T. J. Pedley, *Phys. Rev. Lett.* **100**, 088103 (2008).
- [34] V. Mehandia and P. R. Nott, *J. Fluid Mech.* **595**, 239 (2008).
- [35] N. Sambelashvili, A. W. C. Lau, and D. Cai, *Phys. Lett. A* **360**, 507 (2007).
- [36] K. Drescher, J. Dunkel, L. H. Cisneros, S. Ganguly, and R. E. Goldstein, *Proc. Natl. Acad. Sci. U.S.A.* **108**, 10940 (2011).
- [37] M. F. Copeland, S. T. Flickinger, H. H. Tuson, and D. B. Weibel, *Appl. Environ. Microbiol.* **76**, 1241 (2009).
- [38] L. Turner, R. J. Zhang, N. C. Darnton, and H. C. Berg, *J. Bacteriol.* **192**, 3259 (2010).